Probing the Surface Forces of Monolayer Films with an Atomic-Force Microscope

Nancy A. Burnham, Dawn D. Dominguez, Robert L. Mowery, and Richard J. Colton
Surface Chemistry Branch, Code 6170, Naval Research Laboratory, Washington, D.C. 20375-5000
(Received 8 September 1989)

Using an atomic-force microscope (AFM), we have studied the attractive and adhesive forces between a cantilever tip and sample surfaces as a function of sample surface energy. The measured forces systematically increased with surface energy. The AFM is very sensitive; changes in the surface forces (i.e., attraction and adhesion) of monolayer-covered samples could be clearly discerned when only the surface group of the monolayer film was changed from $-CH_3$ to $-CF_3$.

PACS numbers: 68.35.Md, 62.20.Pn

The atomic-force microscope[1] (AFM) has been used primarily to image the surfaces of insulating materials[2-6] with nanometer-scale resolution. The principal component of an AFM is a small cantilever which measures the force between a tip attached to the cantilever and the surface of interest. The force is determined by multiplying the measured cantilever deflection by the calibrated spring constant of the cantilever. Recording the deflection of the cantilever as a function of sample position generates a force map, or image, of the surface.

Recently, the AFM has also been used to investigate the mechanical properties of materials including atomic-scale friction,[7] elasticity,[8] and surface forces.[8,9] The dependence of the AFM surface-force measurement on tip-sample geometry and materials properties has not been studied systematically until now. In this study, cantilever tip size and shape are measured with a scanning electron microscope before and after use, and the composition, structure, and cleanliness of the sample surfaces are characterized using infrared reflection-absorption spectroscopy. Sample surface energies are determined by contact angle measurements. We measure the attractive and adhesive forces between a tungsten tip and a variety of surfaces, and find the forces detected by AFM increase with sample surface energy. The attractive force results are compared to van der Waals forces calculated for a sphere approaching a flat surface.[10] Derjaguin-Muller-Toporov (DMT) adhesion theory[11,12] is used to analyze the adhesive forces. We estimate the contact area between tip and sample at zero applied load, and discuss the implications for tribology and imaging.

Our instrument employs a "double cross" cantilever which constrains the motion of the tip to the z direction (normal to the sample surface). The cantilever has an effective spring constant of 50 ± 10 N/m and its deflection is measured with a tunneling microscope. The tunneling microscope was operated in the constant-current mode, well below its maximum slew rate. Therefore, the force between the tunneling tip and cantilever was constant, and was ignored in our calculations. Details of the instrumentation are described elsewhere.[8] The AFM measurements were done in a glove box under dry nitrogen. The partial pressure of water in the dry box was determined by dew-point measurements to be less than 1 μm of mercury. This is more than 3 orders of magnitude lower than the humidity required for nanometer capillary condensation.[10] As a result the measured attractive force is assumed to be van der Waals.

The samples were mica, graphite, polytetrafluoroethylene (PTFE), float glass slides coated with 100 nm of aluminum (Evaporated Metal Films, Inc.), and two Langmuir-Blodgett (LB) monolayer films of stearic acid and ω,ω,ω-trifluorostearic acid deposited on the native oxide (Al_2O_3) of the aluminum. The graphite and mica surfaces were prepared by exfoliation in air. The PTFE was cleaned with Sparkleen soap solution and rinsed with triply distilled water. The aluminum films were cleaned in hot methanol and rinsed with triply distilled water until the oxide surface was hydrophilic. LB monolayers were prepared on a Langmuir trough.[13] The stearic acid [$CH_3(CH_2)_{16}COOH$, Lachat Chemicals, Inc., 99.5%] and the ω,ω,ω-trifluorostearic acid [$CF_3(CH_2)_{16}COOH$, Shafrin and Zisman[14]] were spread from n-hexane solutions onto a triply distilled water subphase at 25 °C. The films were compressed and transferred at a film pressure of 20 mN/m.

Equilibrium advancing contact angles were measured on a model A-100 Ramé-Hart goniometer at ambient conditions and the critical surface tensions for wetting, γ_c, were determined by the Fox-Zisman method.[15] In this paper, we assume that γ_c is a close approximation to the sample surface energy, γ_s.[10] The measured surface energies varied from 41 to 21 mJ/m^2, and agreed favorably with literature values (see Table I). We are not able to determine γ_c over 72 mJ/m^2, so instead the γ_s literature values for graphite and mica (exfoliated in air) were used.

Figure 1 shows typical AFM data from four samples. [The graphite and mica data (not shown) look like the data for Al_2O_3, but with much larger cantilever deflections.] The curves depict the forces acting on the

Work of the U. S. Government
Not subject to U. S. copyright

TABLE I. The experimental results for each sample measured with a tungsten tip under dry nitrogen. γ_{lit} and γ_{expt} are the literature and experimental sample surface energies. R is the radius of curvature of the tip as determined by scanning electron microscopy. The maximum attractive and adhesive forces, $|F_{attr}|$ and $|F_{ad}|$, are found by multiplying the respective cantilever deflection, $|\Delta z|$, by the effective spring constant of the cantilever. The forces are then normalized for the tip radius by dividing by $4\pi R$.

	Surface energy		Tip radius	Attractive force			Adhesive force		
Sample	γ_{lit} (mJ/m^2)	γ_{expt} (mJ/m^2)	R (μm)	$\lvert\Delta z\rvert$ (nm)	$\lvert F_{attr}\rvert$ (nN)	$\lvert F_{attr}/4\pi R\rvert$ (mJ/m^2)	$\lvert\Delta z\rvert$ (nm)	$\lvert F_{ad}\rvert$ (nN)	$\lvert F_{ad}/4\pi R\rvert$ (mJ/m^2)
Mica	300,[a] 375[b]	...	2.5 ± 0.5	4.5 ± 0.6	230 ± 30	7.2 ± 1.0	6.6 ± 3.0	330 ± 150	11 ± 5
Graphite	96,[c] 123[d]	...	2.5 ± 0.5	2.5 ± 1.8	140 ± 90	4.5 ± 2.9	4.4 ± 2.4	220 ± 120	7.0 ± 3.8
Al_2O_3	45[e]	41 ± 4	2.0 ± 0.5	1.7 ± 0.5	85 ± 25	3.4 ± 1.0	2.0 ± 0.5	100 ± 25	4.0 ± 1.0
$CH_3(CH_2)_{16}COOH$	21[f]	24 ± 2	2.0 ± 0.5	0.33 ± 0.22	17 ± 11	0.68 ± 0.44	0.70 ± 0.22	35 ± 11	1.4 ± 0.4
$CF_3(CH_2)_{16}COOH$	20[f]	23 ± 2	3.0 ± 0.5	0.10 ± 0.08	5.0 ± 4.0	0.13 ± 0.11	0.39 ± 0.15	20 ± 8	0.53 ± 0.20
PTFE	18[g]	21 ± 2	2.5 ± 0.5	0.04 ± 0.04	2 ± 2	0.06 ± 0.06	0.10 ± 0.10	5.0 ± 5.0	0.16 ± 0.16

[a]Bowden, Ref. 18.
[b]Gregg, Ref. 19.
[c]Fowkes, Ref. 20.
[d]Fowkes, Ref. 21.
[e]Arkles, Ref. 17.
[f]Shafrin and Zisman, Ref. 14.
[g]Shafrin and Zisman, Ref. 22.

cantilever tip as a function of sample position. The measurement starts with the sample far away and the cantilever in its rest position. As the sample is moved towards the cantilever tip, the cantilever bends towards the sample due to attractive surface forces. (For high-surface-energy samples like graphite and mica, the cantilever jumps into contact with the sample once the gradient of the attractive force exceeds the cantilever spring constant.) The maximum forward deflection $|\Delta z|$ of the cantilever multiplied by k is the attractive force for the system. Continuing the forward motion of the sample, the sample pushes the cantilever back through its original rest position until a small load (restricted in this experiment to a maximum applied load of about 100 nN) is applied to the sample by the cantilever. For example, in Fig. 1(a), the sample moves 5 nm while pushing the cantilever 1.5 nm. The subsequent sample deformation of 3.5 nm is consistent with elastic asperity deformation and/or the presence of a thin contamination layer.[16] The slope of the curve in this region will be a function of the elastic moduli and geometries of the tip and sample[8] and will only approach 1 for rigid systems.

The sample direction is now reversed such that it moves away from the cantilever. The cantilever also reverses direction, passing back through its rest position, to the point where the tip and the sample separate (noted when the cantilever changes direction again). The maximum cantilever deflection $|\Delta z|$ during sample retraction multiplied by k is the adhesive force. The results are summarized in Table I. The attractive and adhesive forces were averaged from a minimum of ten runs on separate locations on the samples.

When the surface energy of the Al_2O_3 film is reduced by depositing the LB films, the measured attractive and adhesive forces decrease. By changing only the surface group of the monolayer films from $-CH_3$ to $-CF_3$, the surface forces are modified significantly. This implies that AFM images obtained in the attractive mode using modulation techniques depend on both surface energy and topography. In addition, the shape of the force curves in Figs. 1(b)–1(d) shows a broader minimum compared to the Al_2O_3 data. The flatness of the force curves during the initial stage of compression is most likely a measurement of the elastic modulus of the monolayer films and polymer surface. The slight negative deflection of the cantilever [in Figs. 1(a), 1(c), and 1(d)] just before the cantilever moves towards the sample is worth noting because the feature is fairly reproducible. The origin of the effect is only speculative, however, and requires further study to substantiate.

According to van der Waals force laws,[10] the nonretarded attractive force between a sphere and a flat surface is $F_{attr}=-AR/6D^2$ for $D\ll R$, where A is the Hamaker constant, R is the radius of the sphere, and D is the distance between the sphere and surface. For our samples, A may be evaluated by the equation $A=12\pi D_0^2\Delta\gamma$, where D_0 is ~0.2 nm and $\Delta\gamma$ is equal to $2(\gamma_t\gamma_s)^{1/2}$ (with γ_t is the surface energy of the tip and γ_s is the sample surface energy).[10] Hence, at contact, the maximum attractive force (in the absence of repulsive forces) is $F_{attr}=-4\pi R(\gamma_t\gamma_s)^{1/2}$.

DMT theory for elastic contact[11,12] involves the calculation of the attractive forces outside the contact zone which causes the surfaces to deform according to the Hertz equation. For a small, rigid sphere with low surface energy, the theory shows that, as the surfaces are pulled apart, the maximum force at separation occurs at point contact where the force of adhesion is equal to $-2\pi R\Delta\gamma$ or $-4\pi R(\gamma_t\gamma_s)^{1/2}$. The theory predicts the force to be the same for adhesion or attraction because, as a simplifying assumption, it ignores the attractive interaction within the contact area. The data in Table I show consistently that adhesion is always greater than attraction for each sample. The measured hysteresis in

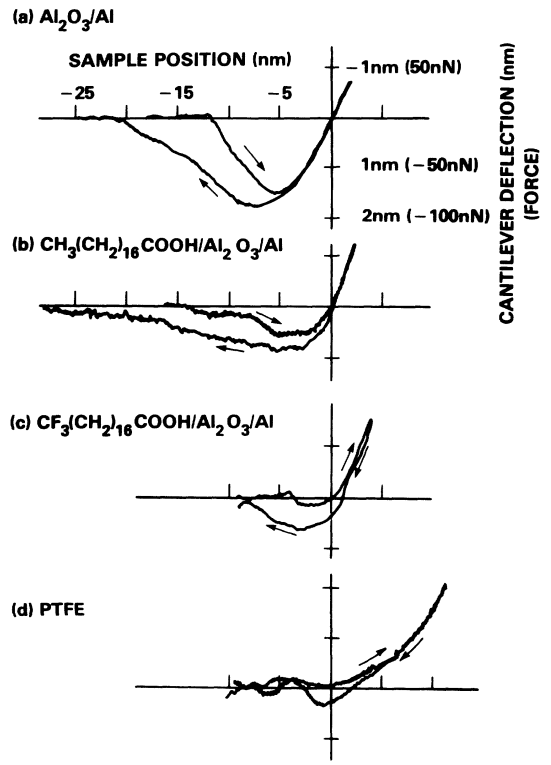

FIG. 1. Representative data obtained with the AFM showing surface-force interaction between a tungsten tip and (a) the native oxide of aluminum (Al_2O_3/Al), (b) stearic acid [$CH_3(CH_2)_{16}COOH$], (c) ω,ω,ω-trifluorostearic acid [CF_3-$(CH_2)_{16}COOH$], and (d) PTFE. The x axis is the sample position in nanometers; the y axis is cantilever deflection in nanometers relative to its rest position, or the force in nanonewtons between the cantilever and sample. The scales for all the curves are the same.

Fig. 1 is a consequence of the adhesive bonding between the tip and sample.

Figure 2 is a log-log plot of the surface forces normalized for tip size, $|F/4\pi R|$, versus sample surface energy, γ_s. The data points for the higher-surface-energy materials (i.e., Al_2O_3, graphite, and mica) show the expected square-root dependence on surface energy as indicated by the dashed line. However, their magnitude is a factor of 10 lower than expected, if a tip surface energy of 100 mJ/m^2 (typical for metal oxides[17]) is assumed. Small asperities on the tip and/or sample could account for this difference in that the measured attractive force would be diminished by minitips with small radii of curvature. The deviation of the lower-surface-energy materials from the square-root dependence may be related to differences in their mechanical properties such as lower elastic modulus and viscoelastic behavior.

DMT adhesion theory also predicts that at zero applied load (when the load is entirely due to surface forces) that there is a finite contact area between the tip and the sample. Assuming a circular contact area as

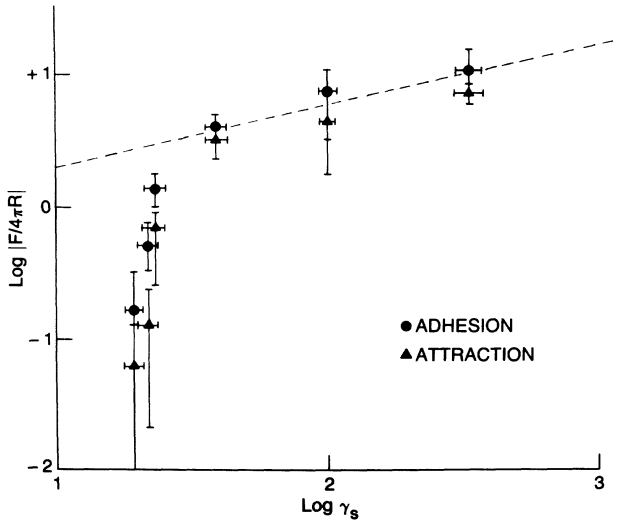

FIG. 2. A log-log plot of $|F/4\pi R|$ for both attraction and adhesion as a function of sample surface energy, γ_s. The dashed line represents the anticipated square-root dependence on the sample surface energy. The error bars correspond to the standard deviations given in Table I.

viewed from above, the radius is

$$a_0 = (2\pi R^2 \Delta\gamma/K)^{1/3},$$

where K depends on the elastic moduli of the tip and sample. We estimate that a_0 was between 10 and 20 nm for our experimental configuration and choice of samples. The term a_0 is important for researchers interested in imaging with the AFM. By choosing small $\Delta\gamma$ and R, and large K (high elastic moduli), it may be possible to achieve single-atom contact at zero applied load. By using a conducting tip, AFM could be used to study the electrical properties of small-area contacts where quantum interference effects may occur.

An estimate of the average pressure under the tip at zero applied load may be obtained by dividing the adhesive forces by the circular contact area πa_0^2. In our system, the pressures varied from 300 MPa for Al_2O_3 to 4 MPa for PTFE. These pressures should be considered when imaging delicate samples. A pressure of 300 MPa is comparable to pressures involved in tribological tests, suggesting that surface forces should be included in tribological modeling at low applied loads.

In conclusion, it is evident that the attraction and adhesion seen with an AFM depends on the sample surface energy, and that the adhesion is always greater. For surface energies at $\sim$40 mJ/m^2 and higher, $|F/4\pi R|$ goes as $\gamma_s^{1/2}$. The instrument can detect relatively large changes in surface forces due to small changes in sample surface energy, suggesting that noncontact AFM imaging depends on both topography and surface energy. The radii of the contact areas at zero applied load were estimated to be 10–20 nm. The average pressures and contact areas under the tip generated by surface forces

should be considered when imaging and in tribology. In addition, the AFM promises to be a useful tool for studying the mechanical properties of monolayers and the electrical properties of nanometer-scale contacts.

The authors thank W. R. Barger and J. L. Dote of the LB film group, and C. Marrian, D. DiLella, R. Brizzolara, S. Brandow, and K. Lee of the STM/AFM group for their suggestions and helpful discussions. This work was done while N.A.B. held a National Research Council–Naval Research Laboratory Associateship.

[1]G. Binnig, C. F. Quate, and Ch. Gerber, Phys. Rev. Lett. **56**, 930 (1986).

[2]O. Marti, B. Drake, and P. K. Hansma, Appl. Phys. Lett. **51**, 484 (1987).

[3]T. R. Albrecht and C. F. Quate, J. Appl. Phys. **62**, 2599 (1987).

[4]T. R. Albrecht, M. M. Dovek, C. A. Lang, P. Grutter, C. F. Quate, S. W. J. Kuan, C. W. Frank, and R. F. W. Pease, J. Appl. Phys. **64**, 1178 (1988).

[5]Y. Martin and H. K. Wickramasinghe, Appl. Phys. Lett. **50**, 1455 (1987).

[6]B. Drake, C. B. Prater, A. L. Weisenhorn, S. A. C. Gould, T. R. Albrecht, C. F. Quate, D. S. Cannell, H. G. Hansma, and P. K. Hansma, Science **243**, 1586 (1989).

[7]C. M. Mate, G. M. McClelland, R. Erlandsson, and S. Chiang, Phys. Rev. Lett. **59**, 1942 (1987); R. Erlandsson, G. Hadzioannou, C. M. Mate, G. M. McClelland, and S. Chiang, J. Chem. Phys. **89**, 5190 (1988).

[8]N. A. Burnham and R. J. Colton, J. Vac. Sci. Technol. A **7**, 2906 (1989).

[9]A. L. Weisenhorn, P. K. Hansma, T. R. Albrecht, and C. F. Quate, Appl. Phys. Lett. **54**, 2651 (1989).

[10]J. N. Israelachvili, *Intermolecular and Surface Forces* (Academic, New York, 1985).

[11]B. V. Derjaguin, V. M. Muller, and Yu. P. Toporov, J. Colloid. Interface Sci. **53**, 314 (1975).

[12]M. D. Pashley, J. B. Pethica, and D. Tabor, Wear **100**, 7 (1984).

[13]W. Barger, J. Dote, M. Klusty, R. Mowery, R. Price, and A. Snow, Thin Solid Films **159**, 369 (1988).

[14]E. G. Shafrin and W. A. Zisman, J. Phys. Chem. **61**, 1046 (1957).

[15]H. W. Fox and W. A. Zisman, J. Colloid. Interface Sci. **5**, 514 (1950).

[16]A. Tonck, J. L. Loubet, and J. M. Georges, ASLE Trans. **29**, 532 (1986).

[17]B. Arkles, Chemtech **1977**, 766.

[18]F. P. Bowden, *Fundamentals of Gas-Surface Interactions* (Academic, New York, 1976), p. 12.

[19]S. J. Gregg, *The Surface Chemistry of Solids* (Reinhold, New York, 1961), p. 139.

[20]F. M. Fowkes, *Chemistry and Physics of Interfaces* (American Chemical Society, Washington, DC, 1971), p. 157.

[21]F. M. Fowkes, *Chemistry and Physics of Interfaces* (Ref. 20), p. 5.

[22]E. G. Shafrin and W. A. Zisman, J. Phys. Chem. **64**, 519 (1960).